

Predominantly extra-retinotopic cortical response to pattern symmetry

Christopher W. Tyler,^{a,*} Heidi A. Baseler,^a Leonid L. Kontsevich,^a
Lora T. Likova,^a Alex R. Wade,^a and Brian A. Wandell^b

^aSmith-Kettlewell Eye Research Institute, San Francisco, CA, USA

^bDepartment of Psychology, Stanford University, Stanford, CA, USA

Received 15 December 2003; revised 26 April 2004; accepted 17 September 2004

Available online 26 November 2004

Symmetry along one or more axes is a key property of objects and biological organisms. We report on a bilateral visual region of occipital cortex that responds strongly to the presence of multiple symmetries in the viewed image. The stimuli consisted of random dots organized in fourfold and onefold mirror-symmetric patterns, against random control stimuli. The contrast between symmetric and random patterns produced negligible or inconsistent activation of the primary visual projection area V1 or of other medial occipital projection areas. However, there was strong symmetry-specific activation in extra-retinotopic lateral occipital cortex. The high level of activation in this region of cortex may represent part of a general class of computations that require integration of information across a large span of the visual field.

© 2004 Elsevier Inc. All rights reserved.

Keywords: Symmetry; Visual perception; fMRI; Brain

Introduction

Visual perception involves a series of synaptic transformations through which visually responsive neurons in the brain process image information projected onto the retina. The spatial integration across the visual scene by cortical neurons can be more than a thousand times greater than for the individual photoreceptors. What analysis do the large receptive fields of these cortical neurons perform?

Several fundamental types of visual computation employ information that is distributed across large portions of the visual field. These computations may be useful for a variety of visual functions, including perceptual rescaling (color constancy), esti-

imating object properties (connectivity, perceptual grouping), and the processing of specific cues that are important for pattern recognition and object classification. Symmetry is an example of an object property that requires long-range integration of scene features. In many cases, symmetry information is not present in the local features and can be found only by comparing information distributed across long distances in the visual field. (Tyler and Hardage, 1996). The reason for the perceptual salience of symmetry is unclear, but it has been argued that symmetry is a useful cue for discriminating living organisms (friend or foe) from inanimate objects. Symmetry has been shown to be a significant determinant of mate selection (Johnstone, 1994; Moller, 1992).

In relation to the evolutionary theme, there is a well-established relationship between symmetry and perceived attractiveness (or beauty) of potential mates in humans, both in their faces (Grammer and Thornhill, 1994; Jacobsen and Hofel, 2002; Mealey et al., 1999; Rhodes et al., 2001, 2002) and in their bodies (Booth et al., 2002; Tovee et al., 2000). Possible confounds of symmetry correlating with masculinity or with familiarity have been ruled out (Little and Jones, 2003; Penton-Voak et al., 2001). Some studies find the opposite effect of a preference for natural asymmetries (Swaddle and Cuthill, 1995) but there is a consensus that the dimension of preference for asymmetry is aligned with emotional expressiveness of the face rather than structural variables, for which symmetry is preferred (Kowner, 1996; Zaidel et al., 1995). Curiously, although symmetry preference in infants is demonstrable for abstract patterns (Fisher et al., 1981; Humphrey and Humphrey, 1989; Humphrey et al., 1986; Pornstein and Krinsky, 1985), any preference for symmetry in faces has been difficult to establish (Rhodes et al., 2002; Samuels et al., 1994).

Taken as a whole, such studies show a strong association between the perception of symmetry and its biological relevance in mate selection for humans, although it is evident that there are competing factors such as emotional expressiveness that also come into play. The importance of symmetry as a visual cue to humans is evident from the widespread occurrence of symmetric patterns and

* Corresponding author. Smith-Kettlewell Eye Research Institute, 2318 Fillmore St., San Francisco, CA 94115, USA. Fax: +1 415 345 8445.

E-mail address: cwt@ski.org (C.W. Tyler).

Available online on ScienceDirect (www.sciencedirect.com).

designs in the constructed environment of architecture and art throughout human history (Tyler, 1996). It is a striking fact of our constructed environment that symmetry is built extensively into furniture, buildings, ornaments, and vehicles. Some of this fabricated symmetry is a reflection of the bilateral symmetry of its users, but much of it has a purely esthetic role. Common examples are oriental rugs and inlaid cabinetry. It is unclear from an evolutionary perspective whether there is an adaptive value for humans to enhance the symmetry around them, but it is clearly a ubiquitous urge whose neural basis is of considerable interest.

There is some neuropsychological evidence of a cortical specialization for large-scale visual computations. Patients suffering from certain visual agnosias, for example simultanagnosia, identify local elements of the visual field but have difficulty discerning the relations among elements in the image. The patients act as though they can see only one object at a time. Brain injury in these patients is often associated with localized lesions in the occipito-parietal portions of the brain (Farah, 1990). More specifically, certain patients with posterior cerebral artery infarcts of the lateral occipital cortex show a specific deficit in detecting bilateral symmetry in random-dot patterns presented to the contralesional visual field, while pattern and motion discrimination in the deficient regions of the field are relatively normal (L. Vaina, personal communication). There is one (and remarkably, only one) study that has reported single-cell responses specific to the presence of symmetric configurations of visual stimuli (Lee et al., 1998). Using shapes specified by the second-order borders between different orientation-defined textures, they found local activations at the point where the shapes lay symmetrically over the receptive fields of neurons in monkey area V1, that is, where the symmetry axis of the figure coincided with the receptive field position defined by the texture-edge response. Although they recorded in V1, these authors concluded from an analysis of the delayed dynamics of the symmetry response that it did not originate in V1 but by feedback from a higher cortical area. Thus, although this lone study identified symmetry as a relevant variable for neural processing in visual cortex, it did not identify the locus at which the property of symmetry is extracted and identified in terms of a neural signal distinct from that for the local pattern elements in the stimulus. The technique of functional Magnetic Resonance Imaging (fMRI) offers the opportunity to track down the cortical region(s) where symmetry-specific processing occurs.

We used fMRI to measure activity in the cortical visual pathways while observers viewed patterns containing large-scale symmetry. The object of the study was to determine whether the

property of symmetry would elicit specialized responses or activate known retinotopic regions of human cortex. Four hypotheses were evaluated:

- (i) that symmetry-specific activation would occur in area V1, where Lee et al. (1998) found symmetry-axis responses in monkey,
- (ii) that symmetry-specific activation would occur in adjacent retinotopic areas, well-positioned to be the source of the feedback signal of Lee et al. (1998),
- (iii) that symmetry-specific activation would occur in higher retinotopic areas known to process pattern structure (such as V3A or V4), and
- (iv) that symmetry-specific activation would occur in further region of occipital cortex whose specialization remains to be determined.

The results showed an increase in fMRI signal in a bilateral region of occipital cortex when the observers viewed fields of random versus symmetric patches in comparison control stimuli of purely random dots. The activity caused by the pattern symmetries was mainly present outside the early visual projection areas V1–V4 (which can be identified by retinotopic mapping with traveling-wave stimuli; DeYoe et al., 1996; Engel et al., 1994, 1997; Sereno et al., 1995).

Materials and methods

Stimuli and experimental procedures

Experiment 1

The stimuli for the primary experiments consisted of 16° fields of white dots, each $15'$ in diameter, at 25% density on a dark background. The primary symmetry probe consisted of fields of random dots organized with symmetry structure alternated in a block design with null sequences of non-symmetric random patterns. Examples are shown in Fig. 1, with a four-axis reflection symmetry pattern in Fig. 1a, and a non-symmetric random pattern in Fig. 1b. Note that very little of the symmetry can be detected by local spatial analyses spanning the size of classical receptive fields found in primary visual cortex, typically less than 0.5° in diameter (Albrecht et al., 1980; Hubel and Wiesel, 1968; Parker and Hawken, 1985). The evident symmetry structure in Fig. 1a is not concentrated at the horizontal, vertical, and oblique axes of

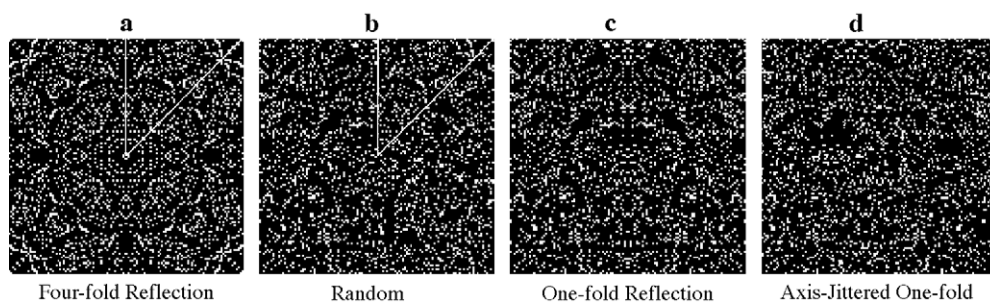


Fig. 1. Examples of individual test stimuli. (a) Four-fold reflection symmetry of a random dot base pattern. (b) Non-symmetric random dot control pattern. The octant triangle of random pattern from which the symmetry pattern was generated is delineated in both a and b. Note that the random pattern in b has just as many feature clumps as in a, but they appear less salient because they lack a symmetric structure. (c) One fold reflection about a vertical axis. (d) Axis-jittered version of c, to mask the axis by random displacement of the lines horizontally without changing the local symmetry structure (see text).

Table 1
Proportion correct in the two-back task for the two pattern types

Observer	LLK	CWT	LTL	LAB
Symmetry patterns	0.87	0.90	0.85	0.76
Random patterns	0.88	0.89	0.85	0.78
Number of trials	1022	774	1162	516

symmetry but at arbitrary positions in the image determined by the perceived contrast energy of the pattern, which has the same range of perceptual strength as in the random pattern of Fig. 1b. The random segment that was used to generate Fig. 1a is delineated as the triangular base element in Fig. 1b. Notice this pattern region is perceived as structured when flanked by its symmetric counterparts, but it is perceived as random when surrounded by other random patterning. Perceptual ratings of the full set of stimuli over four repeats, by four separate observers for the presentation time comparable with that used in the fMRI studies, revealed that symmetry was perceived in 100% of the four-axis stimuli and in 0% of the random stimuli. These stimuli therefore lie at the extremes of the psychometric continuum for symmetry with the presentation time, used (1.5 s per stimulus frame), providing maximum perceptual modulation on the symmetry dimension.

Three observers were tested in a 1.5-T GE Signa scanner and three more in a 3-T GE Signa scanner. For the observers scanned at 1.5 T, the stimulus sequence consisted of an 18-s period of symmetric patterns updated every 1.5 s, alternating with a matching 18-s period of purely random dot patterns. Each 1.5 s frame consisted of 1245 ms of the stimulus interleaved by 255 ms blank periods to block the perception of apparent motion of the dots from one frame to the next. Any residual local motion was, in any case, equated by the use of the same form of base noise for the test and null sequences. The 36 s sequence was repeated six times per scan for a total duration of 216 s per condition.

For the three observers scanned at 3T, the specification of the non-symmetric null stimuli was improved to a Fourier-matched texture. Introducing symmetry into a random pattern does slightly alter the dot statistics, since each dot is replicated eight times (for four-axis symmetry), increasing the variance of the pattern relative to a purely random texture of the same number of dots. To ensure that this difference in the variance properties was not responsible for the observed pattern of activations in the 1.5-T observers, the null stimuli for the 3-T observers were generated by taking the Fourier Transform of each symmetry pattern, randomizing the phase spectrum and then rebinarizing the image to return to the same random-dot density structure. The Fourier-randomized nulls thus had Fourier spectra matched to those of the symmetric test patterns, but with random spatial structure. The variance structure both within the test and null patterns and between the two alternated stimulus sets was now fully equated. The only cue for the observed activations was therefore the configurational property of the symmetry structure compared with the random structure.

Experiment 2

The second experiment controlled both for the type of symmetry and the level of attention to the test and null stimuli. The block design used for Expt. 1 provides a greater signal-to-noise ratio than the more recent event-related paradigms. Having identified a significant response to symmetry, possible attention confounds are addressed by a demanding attention task in Expt. 2.

The attention task was a “two-back” judgment of whether the current image was the same as the image before last, designed to be equally attentionally demanding for randomized as for symmetry patterns. It was also designed to maintain performance at the optimal level on the psychometric function in order to allow evaluation of differences in recognition level between the symmetry and the null random patterns. If the observers could recognize the patterns at the same rate in both conditions, they must have been paying an equal degree of attention to the two stimulus types.¹ To address the possibility that the fourfold symmetry evoked a special kind of shape processing, the stimuli for Exp. 2 were simplified to bilateral symmetry (of otherwise random-dot patterns) around a vertical axis (Fig. 1c). This change provides a test of the generality of the symmetry response, in addition to the attentional control.

For this symmetry control condition, we also incorporated a new kind of null pattern with exactly the same structure as the symmetry pattern on every line, but with successive lines randomly rotated left or right up to half the width of the pattern (Fig. 1d). These axis-randomized stimuli were perceptually indistinguishable from random in every instance. This manipulation amounts to scrambling the location of the symmetry axis line by line, and results in a set of perceptually random patterns with not only the same spatial-frequency content but also the same local symmetry information as the symmetric patterns. The performance on the two-back attention task (Table 1) confirmed that equal attention was being paid to the symmetric and the axis-randomized stimuli. For each of the four observers, performance was matched within 2% for the two conditions, actually slightly favoring the random patterns.

Scanning procedure

The stimuli were rear-projected onto a translucent screen before a 45° mirror inside the bore of the scanner by means of an LCD projector controlled by a Macintosh computer. The observer's head was stabilized either on a bite bar (in the 1.5-T condition) or by temple pads (in the 3-T condition). The observer's task was to maintain fixation on a red 4 × 4 pixel fixation point at the center of the stimulus and to concentrate on the stimulus pattern. No motor

¹ This particular form of attentional control was chosen because it maintains attention to the properties of the pattern in general without specifically focusing on the presence of symmetry in the pattern, but also without distracting attention away from the pattern as an auxiliary task at fixation would do. The two-back recognition task is also superior to a stimulus-relevant task of the form introduced by Huk et al. (2001), for example, in showing that attention-demanding performance is equated for the same task in the two conditions. Huk et al. (2001) incorporated the stimulus-relevant task of speed discrimination in a motion/static fMRI comparison, adjusting the percent correct detection to 75% by increasing the speed of one of two drifting gratings in during the test period or discriminating a slow drift from static during the null period. This paradigm has a possible confound in allowing both the stimulus increment and the observer's performance to covary, and hence not equating the attentional load (although the reported data showed that the stimulus increments were approximately equated in the two conditions). In the two-back task, on the other hand, the stimulus is always presented at full contrast, so the equation of performance strongly implies that attention to the pattern was equated for all observers.

task was imposed, in order to limit the differential brain response to include only sensory processing signals and to avoid confounding the responses with motor or decision processing. Functional magnetic resonance (T2*-weighted, blood oxygenation level dependent, or BOLD) images were collected by means of a figure-eight surface coil in eight planes through the occipital lobes using a 2D spiral sequence (two spiral interleaves, TR = 1500 ms, TE = 40 ms, flip angle = 90°, voxel size = $1 \times 1 \times 4$ mm). For the three further observers tested at 3T, the same conditions were used except with 23 planes, TE = 30 ms and voxel size $0.86 \times 0.86 \times 3$ mm.

Data analysis and visualization

The fMRI (BOLD) response was analyzed by extracting the Fourier fundamental of the time series at every voxel at the stimulus alternation rate of 1/36 Hz. The initial response transient to stimulus onset was excluded by beginning dummy visual stimulation 12 s before the experimental stimulus sequence was initiated. The analysis was limited to a phase window of 0–60° (corresponding to a 6-s window post-stimulus onset). A statistical correction for multiple occurrences was applied by selecting voxels exhibiting coherence level >0.4, which provided a significance level of $P < 0.001$ over the entire set of analyzed voxels in each fMRI slice (i.e., only 0.1% of voxels would produce spurious signals at this correlation level). Note that this means that the probability of adjacent voxels being activated would be $P < 10^{-6}$, so that any clustering of the responses in adjacent voxels represents a highly significant signal.

A high-resolution anatomical (T1-weighted) 3D MRI volume scan of the entire brain was also obtained for each observer (voxel size = $0.94 \times 0.94 \times 1.2$ mm). Gray (cortex) and white (nerve fiber) matter were segmented for each observer using publicly available software (Teo et al., 1997). The differential fMRI activity profile was then mapped directly onto the cortical manifold, to allow visualization of the response properties over complete cortical areas. The boundaries of the retinotopic projection areas V1, V2, V3, V3A, and V4v were established as described in Engel et al. (1997). The V5/MT+ motion complex was identified using an expanding and contracting motion vector field of white dots on a black background, alternating with static dots.

To quantify the comparison of medial retinotopic and dorso-lateral activation for Figs. 3 and 4, we defined anatomical zones that were comparable for the retinotopic and non-retinotopic regions of occipital cortex. To make a fair comparison, we compared symmetry activation within medial and dorsolateral occipital regions specified to be of the same areal size within the flattened cortical manifold (Engel et al., 1997; Teo et al., 1997; Wandell et al., 2000). The medial area was defined retinotopically as the sum of the V1, V2 and V3 from the foveal representation to 16° eccentricity, the size of our stimuli. The matched dorsolateral area was then defined for each observer as a square region of the flattened cortex separated from the border of V3A by 1 cm at the minimum. Within each of the two zones, we then searched for the 4 cm² square area that contained the largest number of voxels reaching the specified criterion of significant activation. Measurement of the distances to other functional activations was based on their published Talairach coordinates and were defined by projection onto the flat-map of the occipital lobe of a typical observer and determination of the shortest distance through cortex as provided by the algorithm developed by Dijkstra (1959) (see Skiena, 1990). This algorithm is implemented in the Stanford

software package of mrLoadRet 3.04, which allows direct computation of the intracortical distance between the two loci in each hemisphere.

Results

Experiment 1

The local hemodynamic response to the symmetry/random alternation was extracted throughout the human occipital lobe and compared with the locations of the retinotopic visual areas obtained by standard fMRI techniques (as described in Materials and methods). In Fig. 2a, a single axial brain slice from passing through the pons, cerebellum, occipital, and temporal lobes is shown for each of three observers scanned at 1.5 T. The slice was chosen to pass through regions of symmetry activation and through retinotopic areas such as V1. The left panels of Fig. 2a show the retinotopic areas in the medial portion of the occipital lobe (multicolor coding). The right panels show fMRI response modulation in the same slices to stimuli alternating between four-axis symmetric and random dot patterns (orange/yellow coding) of the type shown in Figs. 1a and b, respectively. Significant activation was defined by a stimulus/response coherence threshold of 0.40 or above (see Materials and methods). Note that significant activation correlating with the symmetry/random alternation is almost completely absent from the defined retinotopic areas and the human motion-sensitive region, V5/MT+. Instead, activation tends to cluster in bilateral patches of lateral occipital cortex. Each large orange/yellow blob consists of many voxels, each statistically significant at $P < 0.001$. The clustering of adjacent activated voxels thus represents a highly significant response. Note that the levels of 0.4–0.8 shown in Fig. 2 for the correlations with the symmetry sequence also represent correlations with the perceptual symmetry of the stimuli, since behavioral tests indicated that perceived symmetry correlated 100% with the presence of the four-fold symmetry used in this experiment.

Three further observers were run at 3T, using the same four-axis symmetry stimuli but with a Fourier phase-randomized control that equated the Fourier Spectra of the test and null stimuli (see Materials and methods). Results for these observers are shown in surface-rendered images of the occipital lobe and the parietal lobe (Fig. 2b, other details as in Fig. 2a). These data again illustrate that there is a strong symmetry-specific activation localized in the lateral surface of the occipital lobe, well away from the primary retinotopic areas V1–V4 (colored zones in left panels of Figs. 2a and b) but medial and posterior to the motion-specific area, V5/MT+ (Watson et al., 1993; shown in cyan in left panel of Fig. 2a).

To quantify the relative activations in different regions of cortex, we specified medial retinotopic and dorsolateral occipital (DLO) zones of exactly the same size on flattened cortex for each observer and identified the 4 square cm area in each zone that contained the largest number of significantly activated voxels (see Materials and methods). Thus, the retinotopic and non-retinotopic zones had an equal chance of exhibiting symmetry responses on a random basis. Time courses of differential symmetry/random activation are shown for all six observers in Fig. 3. The data depict the summed activation for all significantly activated voxels in the 4 cm² regions showing maximal activation in retinotopic V1 (Fig. 3a) and in the dorsolateral occipital region (Fig. 3b). Clearly,

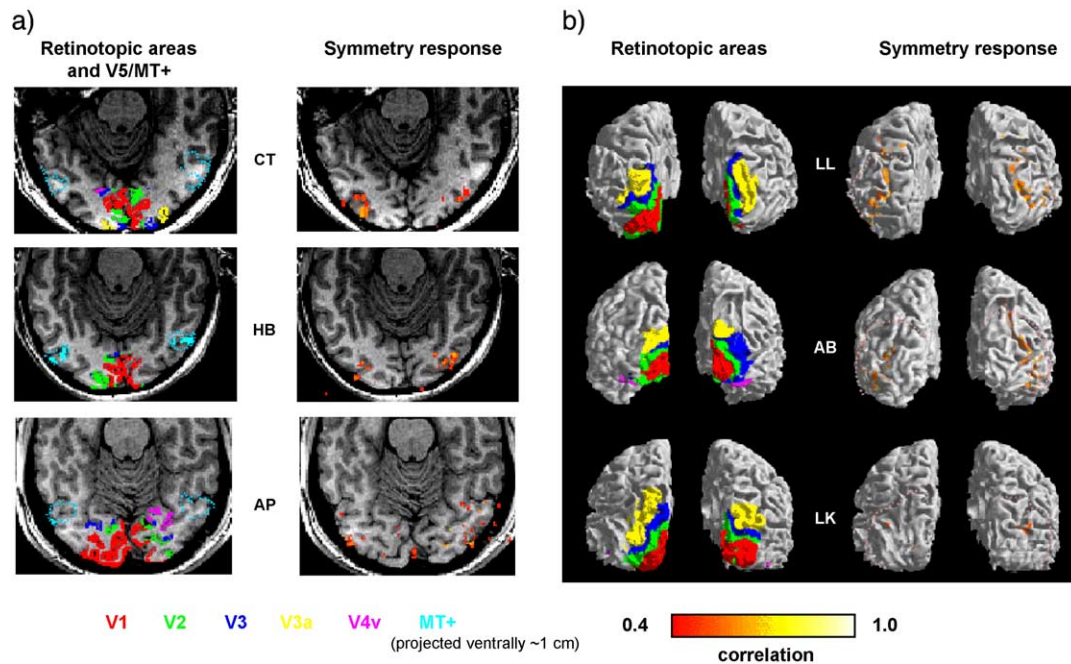


Fig. 2. (a) Axial MRI slices through the occipital lobe comparing retinotopic fMRI activation regions (left panels) with four-axis symmetry activation (right panels) at 1.5 T. Colored regions indicate locations of established visual areas: V1 (red), V2 (green), V3 (blue), V3A (yellow), V4v (magenta) and V5/MT+ (cyan). The center of the V5/MT+ complex is located approximately 1 cm above the slice shown in observers CT and AP, as indicated by the dashed cyan line. Symmetry response correlation level ran from 0.40 to 1.00 (orange > yellow > white). Note that the presence of symmetry evokes negligible activation in any of the retinotopic areas or V5/MT+. (b) Posterior-view renderings comparing retinotopic fMRI activation regions (left panels) with four-axis symmetry activation (right panels) at 3T. The estimated occipitoparietal junctions in each hemisphere are indicated by pink dashed boundaries. The predominant activation by the appearance of symmetry is restricted to lateral occipital regions, with minor extension to parietooccipital regions in some cases.

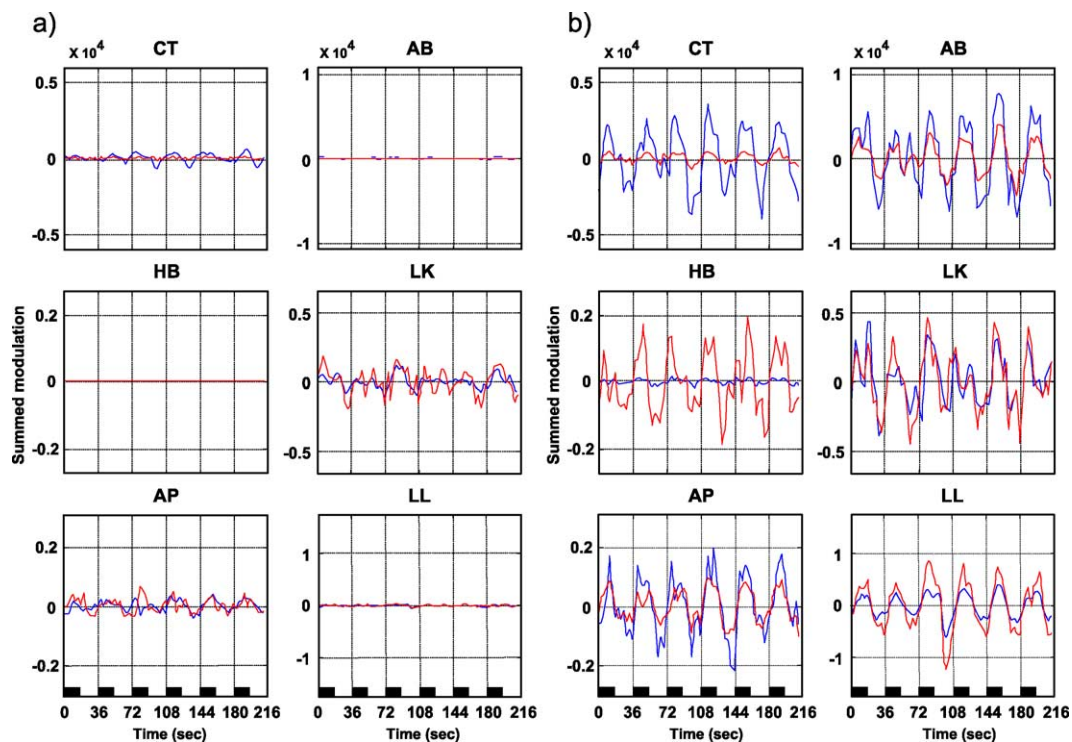


Fig. 3. Summed time series for all significantly activated voxels in retinotopic V1 and a dorsolateral occipital area around the middle occipital gyrus for right (red) and left (blue) hemispheres of six observers (denoted by their initials). Black bars at bottom denote the stimulus presentation times. To have comparable measures, each evaluation is restricted to the 4 cm^2 square of flattened cortex with the largest number of significant activations. (a) Summed responses from area V1. Left panels: 1.5 T scans; right panels: 3T scans. (b) Summed dorsolateral cortex responses. Left panels: 1.5 T scans; right panels: 3 T scans.

Table 2
ANOVA for the ROI voxel-count analysis

	<i>df</i>	<i>F</i>	<i>P</i>
ROI	2	19.59	<0.0000
Hemisphere	1	0.02	0.90
Interaction	2	0.28	0.76

the total activation was much larger in the dorsolateral occipital region than in V1 in all 12 hemispheres tested. Most observers showed similar summed amplitudes in the two hemispheres. Of the two that were asymmetric (CT and HB), the asymmetries complement each other. For good measure, we also report the best symmetry activation in any 4 cm² region of retinotopically defined V3A and V4v at the dorsal and ventral extremes of the retinotopic sequence, although anatomical boundary limitations precluded matching the sizes of these areas.

Statistical evaluation was performed on the number of significantly activated voxels, normalized to the total number of voxels activated in all the regions recorded as a complete set over all six observers (i.e., areas V1–V3, V3A and the DLO area). The automated analysis showed that in each hemisphere significantly more voxels were activated by the four-axis symmetry property in (non-retinotopic) lateral than in any (retinotopic) medial occipital region of matched size. A two-way ANOVA on the ROIs with complete statistics (V1–V3, V3A, and the DLO area) shows that there is a significant main effect of cortical locus ($F(2,1) = 11.8$, $P < 0.01$), but no significant effect of hemisphere or interaction at $P > 0.1$ (Table 2). A Tukey–Kramer comparison of the means shows that the DLO activation is significantly larger than the activation in any other locus tested and than none of the other loci differ from each other or from zero activation ($P > 0.05$).

The locus of symmetry activation was quite stable across observers, as is quantified by means of the Talairach coordinate system (Talairach and Tournoux, 1988). The mean and standard error of the mean (SEM) coordinates are provided in Table 3 for the center of the 2 × 2 cm area most activated by symmetry. The distances in mm are commensurate typical head in Talairach coordinates. Remarkably, the variation over our six observers averaged only about 2.5 mm for each coordinate. There was thus tight agreement as to the occipital locus of maximum activation by this particular pattern property (the modal symmetry locus). It should be emphasized that, although this modal symmetry locus is the only area of those quantified that shows a consistent response to symmetry, we have no evidence in this initial study as to what other stimuli may activate this same area. The table includes

several coordinates from other studies (Amedi et al., 2002; Gilaie-Dotan et al., 2002) for consideration in Discussion.

It is important to note that, in addition to its absence in retinotopic occipital cortex, only weak activation to the symmetry/random contrast was evident in parietal cortex (Fig. 2b). To quantify this comparison, we focused on Brodmann area 40 in parietal cortex that is established as being particularly involved in attentional control (Martinez et al., 1999; Mesulam, 1999). This region has Talairach coordinates RH 28, –49, 47 and LH –29, –55, 50. The number of activated voxels for the 4-cm² area around this coordinate in each of the three 3T observers is shown as the last bar for each hemisphere in Fig. 4. Evidently, there was negligible activity at this location in either hemisphere for any of the three observers. The lack of BA 40 activation rules out the idea that the symmetry activation was either a general attentional signal from the parietal attentional control area or a spatial manipulation signal as observers made mental (or eye movement) comparisons between matching regions of the textures. These characteristics make it clear that the symmetry activation that we describe is not merely a subclass of these well-known response complexes, but a specific locus to which the property of symmetry is of particular interest.

Experiment 2

There is a concern that there may be some other attentional confound, that the activated regions in the DLO characterized in Fig. 4 may represent some kind of unsuspected attentional response rather than activation specific to neural symmetry processing. To address this concern, we ran new scans with an attentional task, unrelated to the presence of symmetry that could equate attention in the two stimulus phases (see Materials and methods).

The symmetry/random fMRI responses were compared in regions of interest (ROIs) defined retinotopically in each hemisphere, in the human motion area (V5/hMT+) defined by a standard motion localizer, and in the topologically defined rectangular region in the DLO. The results of the attention-equated control in the four observers are plotted in Fig. 5 for the percent modulation in voxels whose coherence level exceeded the criterion level of 0.4, normalized to the area of the cortex in which each assessment was conducted. Thus, cortical regions constituting a larger number of voxels would need to show a proportionately larger level of activation to generate the same normalized signal in Fig. 5. The results of this normalized analysis were similar to the original study with passive fixation, that there was a highly

Table 3
Distance of modal symmetry locus from related loci

Study	Hemisphere	Sagittal	Coronal	Axial	Distance from symmetry locus
Modal symmetry locus	L	–34.7	–84.5	–0.7	
	SEM	–3.4	–2.9	–2.7	
	R	31.0	–80.8	2.0	
	SEM	–1.8	–2.0	–3.0	
Gilaie-Dotan LO	L	–41.0	–78.0	–8.8	15.0
	R	40.8	–68.0	–4.5	25.5
Dorsal shape (shape vs. flat)	L	–22.0	–72.0	31.0	26.6
	R	25.5	–72.5	29.3	25.6
Amedi et al. Dorsal LO	L	–28.4	–77.8	–2.5	60.5
	R	33.9	–74.7	–1.0	51.1

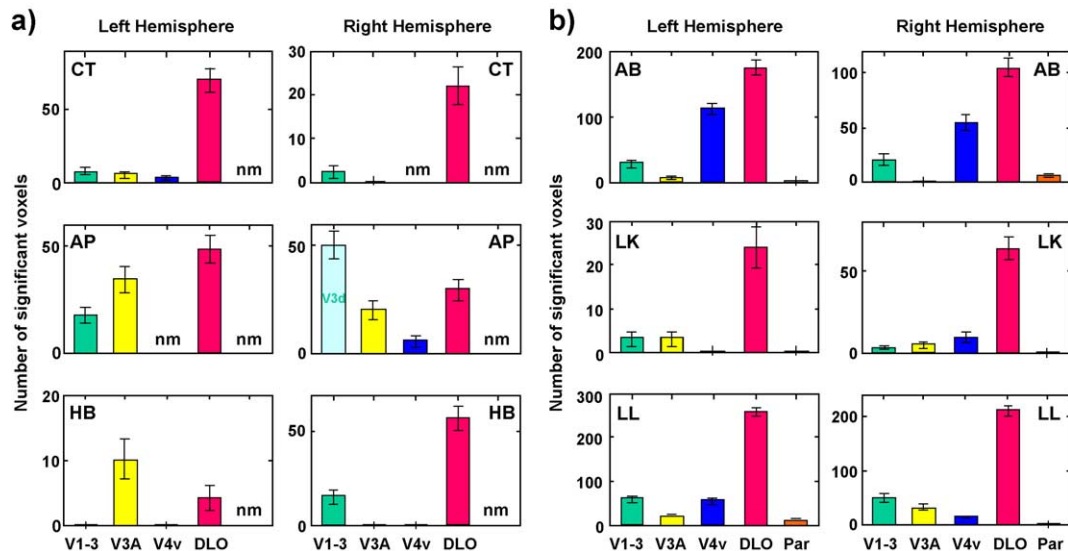


Fig. 4. Bars denote total number of voxels significantly activated by the symmetry/random alternation in the most activated 4 sq. cm of cortex within matched areas in several occipital regions. The cortical regions surveyed were medial retinotopic areas V1–3 and equal-size regions of dorsolateral (DLO) and parietal (Par) cortex (as in Fig. 3, see Materials and methods). For areas V3A and V4v, located dorsally and ventrally in the occipital lobes, respectively, the 4 cm² region of greatest activation was chosen with no attempt to equate the size of the selected regions. Note that the greatest activation density occurred in dorsolateral cortex in 10 of the 12 hemispheres analyzed. The error bars represent \pm one standard error based on a binomial distribution. (a) Data for three observers run at 1.5 T using symmetry alternated with random nulls. Because of limited number of slices, area V4v was not measured (nm) for CT/RH and AP/LH, and signals for parietal cortex were not measured in any hemisphere. (b) Data for three observers run at 3 T using symmetry alternated with Fourier-equated nulls. These panels include a bin (Par) for number of voxels activated in the posterior parietal attentional focus. See Materials and methods for details.

significant signal in the rectangular region in the DLO. A two-factor ANOVA of the group results gave the results specified in Table 4, that the only significant effect was the main effect of over the different ROIs.

Tukey–Kramer post-analyses of the individual means ($P < 0.05$) revealed that the largest symmetry/scrambled activation in the attention-equated condition (normalized to cortical area) was in the DLO in both hemispheres, and this response did not differ significantly between the hemispheres (compare Fig. 5). This analysis showed that there was no statistically significant activation in any retinotopic area in either hemisphere and that the DLO activation was significantly stronger than that in any other area in the right hemisphere. In the left hemisphere, the picture was similar with the DLO activation significantly stronger than in all other regions except for V5 and V3A. We conclude that for both hemispheres the predominant response to symmetry is in the DLO region, although there may be weaker activation in some of the retinotopic areas that could be revealed in a more extensive study.

Discussion

The data are consistent with the idea that regions in the DLO are particularly involved in the processing of long-range stimulus structure. Because there is little symmetry-related activity in the early retinotopic organized visual areas, the responses cannot be explained by the long-range connections present in area V1 (see Callaway, 1998, for a review), area V2 (Merigan et al., 1993; von der Heydt and Peterhans, 1989), or other retinotopic areas (Reppas et al., 1997) (with the individual exceptions noted above). Instead, the symmetry-specific responses imply the existence of neurons with larger receptive fields that are driven by patterns of activity spread across the mosaic of neurons in earlier visual areas. The role of the DLO in long-range visual processing is supported by studies that found a nearby and perhaps overlapping occipital region with a large representation of the ipsilateral visual field (Tootell et al., 1998). Lateral occipital regions including the DLO have also been implicated in the processing of illusory contours (Hirsch et al., 1995; Mendola et al., 1999) and also in the detection of motion

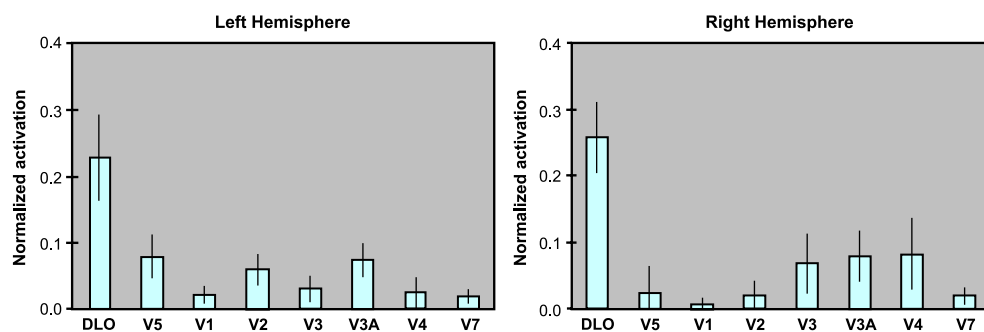


Fig. 5. Mean normalized activations over eight hemispheres in the DLO and each of seven retinotopic cortical regions (including the motion area V5/hMT+) to the symmetry/scrambled comparison with an attention-matching task performed during the scans.

Table 4
ANOVA for the attention-equated ROI analysis

	<i>df</i>	<i>F</i>	<i>P</i>
ROI	7	11.8	<0.0000
Hemisphere	1	0.16	0.69
Interaction	7	0.76	0.62

boundaries (Van Oostende et al., 1997). The ability to identify both symmetry and motion boundaries benefits from the long-range integration of visual information.

One interpretation of the symmetry task is that symmetry stimuli may be expected to elicit local, attentional activation. This activation might be of two kinds: retinotopic or functionally specific. The local retinotopic activation due to attention being drawn to the most interesting area of the stimulus would necessarily show up in retinotopic areas, perhaps to a greater extent in those higher in the hierarchy. However, even without the attentional control, our symmetry/random comparisons generate almost no differential activation in any of the retinotopic areas. The pronounced activations in the DLO symmetry region (which itself shows little retinotopic response) (DeYoe et al., 1996; Sereno et al., 1995; Tootell et al., 1996) cannot be unsuspected retinotopic activations because they remain when attention is equated with the two-back task. The data therefore do not support the interpretation that the DLO symmetry response is any retinotopic form of attentional activation.

The other attentional interpretation could be that the DLO is the control region for the attentional activation, a function often associated with the posterior parietal cortex. Whenever any visual stimulus activates one or more of the retinotopic areas, such hypotheses assume that attentional control would be activated to direct attention to that sensory activity. It would thus show up in an fMRI study as a secondary, non-specific site of activation. Evaluation of the activity in the parietal attentional zone (BA 40) revealed almost no voxels activated by the presence of symmetry (Fig. 4, right bars), so the functionally specific concept of attentional control is not supported either.

Concern may arise that there may be some other attentional confound, such that the activated areas in the DLO characterized in Fig. 4 may be some kind of unsuspected attentional response rather than activation specific to neural symmetry processing. Since the previous two paragraphs have shown that the lateral cortex is neither the source nor the focus of attentional modulation, it is hard to see how generic attention would be involved. The only possibility is that the symmetry structure was actually processed in another cortical location which activated centers of general ‘interest’ that were especially responsive in the presence of some attention-getting stimulus. The passive fixation conditions of the main experiment could reflect this ‘interest’ factor rather than the specific neural processing for the symmetry property per se. This concern is addressed by the scans of Exp. 2 with the difficult two-back task that equated attention to the pattern structure of the stimulus, whether it was symmetric or asymmetric. The results (Fig. 5 and Table 4) provide a complete replication of the main study, with the DLO being the only region strongly activated by the symmetry in relation to scrambled stimuli. Since the performance in the two-back task attention required equal attention in order to equate performance, these results provide assurance that the DLO response was specific to the neural processing of symmetry.

These controls establish that the clear-cut activation found predominantly beyond the primary retinotopic areas is attributable

to the property of symmetry, abstracted from all other stimulus properties by the contrast with matched randomized patterns. This result is important because many studies of stimuli such as objects and faces find activation in the DLO area that they attribute to object processing. By identifying symmetry as a property of cortical activation (and excluding attentional differences as a confound in such responses), the present study begins the analysis of object processing into its component elements. It is a large project to identify all these elements and determine whether they have distinct cortical loci, but a beginning may be made by comparing the Talairach coordinates of the symmetry activation with those of other object properties.

For example, the lateral occipital object-responsive area (LO) defined by Gilaie-Dotan et al. (2002) is anteroventral to the site of maximum symmetry activation and separated by distances of about 2.6 ± 0.25 cm across the cortical surface in the two hemispheres. The distances to the Dorsal LO area defined by Amedi et al. (2002) are similar (Table 3). The symmetry response therefore appears to be coincident with the dorsal arm of the more general object-processing functions. Another candidate area for the symmetry response might be the dorsal shape area reported in Gilaie-Dotan et al. (2002), which did not involve generic objects but the abstracted property of 3D vs. 2D shape. The distances to this area, however, are of the order of 5 cm (Table 3), so it definitely appears to be a functional locus different from that for symmetry processing. While these comparisons make it very clear that the peak symmetry response is not co-localized with the shape response, it seems likely that such symmetry activation locus may be a component of some LO activations. In interpreting such overlap, it should be borne in mind that, while most objects exhibit structural symmetries, random-dot symmetry patterns contain little in the way of object structure. Any overlap found between the object-specific and symmetry-specific response areas therefore implies that studies of object identification need tighter definitions of what is meant by objects versus non-objects, with control of potentially confounding factors such as symmetry and depth.

In conclusion, this initial evaluation of cortical processing of symmetry establishes that symmetry/non-symmetry alternation is a sufficient stimulus for significant fMRI activation in a still poorly-understood region of the human lateral occipital cortex. The high level of activation in the DLO may represent part of a general class of computations that require integration of information across a large span of the visual field. These observations provide an approach to the exploration of the corresponding long-range processing in homologous areas of other species by classic neurophysiological and neuroanatomical techniques.

Acknowledgments

Supported by NEI R01 13025 and the Radiology Department, Stanford University.

References

- Albrecht, D.G., De Valois, R.L., Thorell, L.G., 1980. Visual cortical neurons are bars or gratings the optimal stimuli? *Science* 207, 88–90.
- Amedi, A., Jacobson, G., Hendler, T., Malach, R., Zohary, E., 2002. Convergence of visual and tactile shape processing in the human lateral occipital complex. *Cereb. Cortex* 12, 1202–1212.
- Booth, A.E., Bertenthal, B.I., Pinto, J., 2002. Perception of the symmetrical patterning of human gait by infants. *Dev. Psychol.* 38, 554–563.

- Callaway, E., 1998. Local circuits in primary visual cortex of the macaque monkey. *Annu. Rev. Neurosci.* 21, 47–74.
- DeYoe, E.A., Carman, G.J., Bandettini, P., Glickman, S., Wieser, J., Cox, R., Miller, D., Neitz, J., 1996. Mapping striate and extrastriate visual areas in human cerebral cortex. *Proc. Natl. Acad. Sci.* 93, 2382–2386.
- Dijkstra, E.W., 1959. A note on two problems in connection with graphs. *Numer. Math.* 1, 269–271.
- Engel, S.A., Rumelhart, D.E., Wandell, B.A., Lee, A.T., Glover, G.H., Chichilnisky, E.J., Shadlen, M.N., 1994. fMRI of human visual cortex. *Nature* 369, 525.
- Engel, S.A., Glover, G.H., Wandell, B.A., 1997. Retinotopic organization in human visual cortex and the spatial precision of functional MRI. *Cereb. Cortex* 7, 181–192.
- Farah, M.J., 1990. *Visual Agnosia*. MIT Press Cambridge, Massachusetts. Chapt. 2.
- Fisher, C.B., Ferdinandsen, K., Bornstein, M.H., 1981. The role of symmetry in infant form discrimination. *Child Dev.* 52, 457–462.
- Gilaie-Dotan, S., Ullman, S., Kushnir, T., Malach, R., 2002. Shape-selective stereo processing in human object-related visual areas. *Hum. Brain Mapp.* 15, 67–79.
- Grammer, K., Thornhill, R., 1994. Human (*Homo sapiens*) facial attractiveness and sexual selection: the role of symmetry and averageness. *J. Comp. Psychol.* 108, 233–242.
- Hirsch, J., DeLaPaz, R.L., Relkin, N.R., Victor, J., Kim, K., Li, T., Borden, P., Rubin, N., Shapley, R., 1995. Illusory contours activate specific regions in human visual cortex. Evidence from functional magnetic resonance imaging. *Proc. Natl. Acad. Sci. U. S. A.* 92, 6469–6473.
- Hubel, D.H., Wiesel, T.N., 1968. Receptive fields and functional architecture of monkey striate cortex. *J. Physiol. (London)* 195, 215–243.
- Huk, A.C., Ress, D., Heeger, D.J., 2001. Neuronal basis of the motion aftereffect reconsidered. *Neuron* 32, 161–172.
- Humphrey, G.K., Humphrey, D.E., 1989. The role of structure in infant visual pattern perception. *Can. J. Psychol.* 43, 165–182.
- Humphrey, G.K., Humphrey, D.E., Muir, D.W., Dodwell, P.C., 1986. Pattern perception in infants: effects of structure and transformation. *J. Exp. Child Psychol.* 41, 128–148.
- Jacobsen, T., Hofel, L., 2002. Aesthetic judgments of novel graphic patterns: analyses of individual judgments. *Percept. Mot. Skills* 95, 755–766.
- Johnstone, R.A., 1994. Female preference for symmetrical males as a by-product of selection for mate recognition. *Nature* 372, 172–175.
- Kowner, R., 1996. Facial asymmetry and attractiveness judgment in developmental perspective. *J. Exp. Psychol. Hum. Percept. Perform.* 22, 662–675.
- Lee, T.S., Mumford, D., Romero, R., Lamme, V.A., 1998. The role of the primary visual cortex in higher level vision. *Vis. Res.* 38, 2429–2454.
- Little, A.C., Jones, B.C., 2003. Evidence against perceptual bias views for symmetry preferences in human faces. *Proc. Roy. Soc. Lond., Ser. B* 270, 1759–1763.
- Martinez, A., Anllo-Vento, L., Sereno, M.I., Frank, L.R., Buxton, R.B., Dubowitz, D.J., Wong, E.C., Hinrichs, H., Heinze, H.J., Hillyard, S.A., 1999. Involvement of striate and extrastriate visual cortical areas in spatial attention. *Nat. Neurosci.* 2, 364–369.
- Mealey, L., Bridgstock, R., Townsend, G.C., 1999. Symmetry and perceived facial attractiveness: a monozygotic co-twin comparison. *J. Pers. Soc. Psychol.* 76, 151–158.
- Mendola, J.D., Dale, A.M., Fischl, B., Liu, A.K., Tootell, R.B.H., 1999. The representation of illusory and real contours in human visual cortical areas revealed by functional magnetic resonance imaging. *J. Neurosci.* 19, 8560–8572.
- Merigan, W.H., Nealey, T.A., Maunsell, J.H., 1993. Visual effects of lesions of cortical area V2 in macaques. *J. Neurosci.* 13, 3180–3191.
- Mesulam, M.M., 1999. Spatial attention and neglect: parietal, frontal and cingulate contributions to the mental representation and attentional targeting of salient extrapersonal events. *Phil. Trans. R. Soc. Lond., Ser. B* 354, 1325–1346.
- Moller, A.P., 1992. Female swallow preferences for symmetrical male sexual ornaments. *Nature* 357, 238–240.
- Parker, A., Hawken, M., 1985. Capabilities of monkey cortical cells in spatial-resolution tasks. *J. Opt. Soc. Amer. A* 2, 1101–1114.
- Penton-Voak, I.S., Jones, B.C., Little, A.C., Baker, S., Tiddeman, B., Burt, D.M., Perrett, D.I., 2001. Symmetry, sexual dimorphism in facial proportions and male facial attractiveness. *Proc. Roy. Soc. Lond., Ser. B* 268, 1617–1623.
- Pornstein, M.H., Krinsky, S.J., 1985. Perception of symmetry in infancy: the salience of vertical symmetry and the perception of pattern wholes. *J. Exp. Child Psychol.* 39, 1–19.
- Reppas, J.B., Niyogi, S., Dale, A.M., Sereno, M.I., Tootell, R.B.H., 1997. Representation of motion boundaries in retinotopic human visual cortical areas. *Nature* 388, 175–179.
- Rhodes, G., Yoshikawa, S., Clark, A., Lee, K., McKay, R., Akamatsu, S., 2001. Attractiveness of facial averageness and symmetry in non-western cultures in search of biologically based standards of beauty. *Perception* 30, 611–625.
- Rhodes, G., Geddes, K., Jeffery, L., Dziurawiec, S., Clark, A., 2002. Are average and symmetric faces attractive to infants? Discrimination and looking preferences. *Perception* 31, 315–321.
- Samuels, C.A., Butterworth, G., Roberts, T., Graupner, L., Hole, G., 1994. Facial aesthetics: babies prefer attractiveness to symmetry. *Perception* 23, 823–831.
- Sereno, M.I., Dale, A.M., Reppas, J.B., Kwong, K.K., Belliveau, J.W., Brady, T.J., Rosen, B.R., Tootell, R.B.H., 1995. Borders of multiple visual areas in humans revealed by functional magnetic resonance imaging. *Science* 268, 889–893.
- Skiena, S., 1990. Dijkstra's algorithm. §6.1.1 in *Implementing Discrete Mathematics: Combinatorics and Graph Theory with Mathematica*. Addison-Wesley, Reading, MA, pp. 225–227.
- Swaddle, J.P., Cuthill, I.C., 1995. Asymmetry and human facial attractiveness: symmetry may not always be beautiful. *Proc. R. Soc. Lond., Ser. B* 261, 111–116.
- Talairach, J., Tournoux, P., 1988. *Co-Planar Stereotaxic Atlas of the Human Brain*. Thieme Medical Publishers, New York.
- Teo, P.C., Sapiro, G., Wandell, B.A., 1997. Creating connected representations of cortical gray matter for functional MRI visualization. *IEEE Trans. Med. Imaging* 16, 852–863. <http://white.stanford.edu>.
- Tootell, R.B.H., Dale, A.M., Sereno, M.I., Malach, R., 1996. New images from human visual cortex. *Trends Neurosci.* 19, 818–824.
- Tootell, R.B.H., Mendola, J.D., Hadjikhani, N.K., Liu, A.K., Dale, A.M., 1998. The representation of the ipsilateral visual field in human cerebral cortex. *Proc. Natl. Acad. Sci. U. S. A.* 95, 818–824.
- Tovee, M.J., Tasker, K., Benson, P.J., 2000. Is symmetry a visual cue to attractiveness in the human female body? *Evol. Hum. Behav.* 21, 191–200.
- Tyler, C.W., 1996. *The Perception of Symmetry and its Computational Analysis*. Erlbaum, New Jersey. Reprinted 2003.
- Tyler, C.W., Hardage, L., 1996. Mirror symmetry detection: predominance of second-order pattern processing throughout the visual field. In: Tyler, C.W. (Ed.), *Human Symmetry Perception and Its Computational Analysis*. VSP BV, Zeist, The Netherlands, pp. 157–172.
- Van Oostende, S., Sunaert, S., Van Hecke, P., Marchal, G., Orban, G.A., 1997. The kinetic occipital (KO) region in man: an fMRI study. *Cereb. Cortex* 7, 690–701.
- von der Heydt, R., Peterhans, E., 1989. Mechanisms of contour perception in monkey visual cortex. I. Lines of pattern discontinuity. *J. Neurosci.* 9, 1731–1748.
- Wandell, B.A., Chial, S., Backus, B.T., 2000. Visualization and measurement of the cortical surface. *J. Cog. Neurosci.* 12, 730–752.
- Watson, J.D., Myers, R., Frackowiak, R.S., Hajnal, J.V., Woods, R.P., Mazziotta, J.C., Shipp, S., Zeki, S., 1993. Area V5 of the human brain: evidence from a combined study using positron emission tomography and magnetic resonance imaging. *Cereb. Cortex* 3, 79–94.
- Zaidel, D.W., Chen, A.C., German, C., 1995. She is not a beauty even when she smiles: possible evolutionary basis for a relationship between facial attractiveness and hemispheric specialization. *Neuropsychologia* 33, 649–655.